UC Irvine
UC Irvine Previously Published Works

Title
Structural comparison of the plant satellite viruses.

Permalink
https://escholarship.org/uc/item/3mf1p69f

Journal
Virology, 214(2)

ISSN
0042-6822

Authors
Ban, N
Larson, SB
McPherson, A

Publication Date
1995-12-01

DOI
10.1006/viro.1995.0068

Copyright Information
This work is made available under the terms of a Creative Commons Attribution License, availalbe at https://creativecommons.org/licenses/by/4.0/

Peer reviewed

eScholarship.org Powered by the California Digital Library
University of California

VIROLOGY 214, 571–583 (1995)

Structural Comparison of the Plant Satellite Viruses

NENAD BAN, STEVEN B. LARSON, and ALEXANDER McPHERSON[1]

Department of Biochemistry, University of California at Riverside, Riverside, California 92521

Received August 10, 1995; accepted October 11, 1995

Detailed structures are now available for three plant satellite viruses, satellite tobacco necrosis virus (STNV), satellite tobacco mosaic virus (STMV), and satellite panicum mosaic virus (SPMV). It is, therefore, possible to compare the tertiary structure of viral protein subunits, their quaternary interactions, and the interactions of protein subunits with the RNA genome. This analysis indicates that, in spite of common function and preservation of a "jelly-roll" motif in the protein monomer, the three viruses are remarkably different. The differences include the arrangement of secondary structural elements, interactions of adjacent subunits, and the disposition of subunits relative to icosahedral symmetry axes. In each of the three viruses, however, the narrow end of the jelly roll forms fivefold contacts. The fivefold protein interactions are organized about a Ca^{2+} ion for STNV, an anion for STMV, and, apparently, neither of these for SPMV. Low-resolution neutron diffraction studies using H_2O/D_2O solvent contrast variation revealed the general location of the RNA genome within the STNV. In the case of SPMV, regions of electron density on the interior of the capsid could be assigned to RNA, although it was not possible to model the nucleic acid. Only for STMV was nucleic acid visible in election density maps, and this was manifested as double-helical RNA segments associated with each coat protein dimer. The observations presented here provide no support for any common evolutionary relationship. © 1995 Academic Press, Inc.

INTRODUCTION

Satellite viruses are so named because they cannot replicate in the absence of a helper virus upon which they depend for enzymatic assistance. They are different from satellite RNAs or viroids because they code for a protein which serves to encapsidate the genomic nucleic acid. All are host specific and specific as well for their required helper virus.

There are four well-characterized, protein-encapsidated, satellite viruses of plants, each of $T = 1$ icosahedral symmetry and having a diameter of about 170 Å (reviewed by Pritsch and Mayo, 1989). The viruses are satellite tobacco necrosis virus (STNV; Kassanis, 1962), satellite tobacco mosaic virus (STMV; Valverde and Dodds, 1986; Dodds, 1991), satellite panicum mosaic virus (SPMV; Masuta *et al.,* 1987), and satellite maize white line mosaic virus (SMWLMV; Zhang *et al.,* 1991). These have as their helper viruses tobacco necrosis virus, tobacco mosaic virus, panicum mosaic virus (PMV), and maize white line mosaic virus, respectively. The host plants for the first two helper–satellite pairs are chiefly tobacco; for the PMV–SPMV pair it is millet and for the last case maize. The satellite viruses can replicate in their host cells only when they are co-infected with their helper virus (Francki, 1985; Zhang *et al.,* 1991). The $T = 1$ viruses have 60 subunits related by perfect icosahedral symmetry, implying that the conformations and environments of the subunits are identical (Caspar and Klug, 1962).

The structure of STNV was solved about 15 years ago in the Strandberg laboratory (Liljas *et al.,* 1982; Jones and Liljas, 1984). The structures of STMV and, most recently, SPMV have been solved and refined in our own laboratory to resolutions of 1.8 and 1.9 Å, respectively (Larson *et al.,* 1993a,b; S. B. Larson and A. McPherson, unpublished results; Ban and McPherson, 1995). Although all three structures are known, no detailed comparison of their features has been made.

These viruses have a genome size of 1239, 1059, and 850 nucleotides and capsid protein molecular weights of 21,000, 17,500, and 17,000 daltons, respectively (Pritsch and Mayo, 1989). The structure of the largest $T = 1$ plant satellite virus, SMWLMV, is still unknown. The genome of this virus consists of 1168 nucleotides and encodes for a 208-amino-acid protein with a calculated molecular weight of 23,961 daltons (Zhang *et al.,* 1991). All four viruses contain single-stranded RNA, but the RNAs show a very high propensity for base pairing and likely exhibit an extensive secondary structure with a substantial double-helix content. This can be calculated using the program FOLD (Devereux *et al.,* 1984) employing the algorithm of Zucker and Stiegler (1981).

Although superficially similar in size, appearance, and composition, none of the satellite viruses show any immuno-cross-reactivity with each other, nor is there any significant amino acid or nucleotide sequence homology among them. None shows any immuno-cross-reactivity with its own helper virus, nor shows any substantial ho-

[1] To whom reprint requests should be addressed.

0042-6822/95 $12.00
Copyright © 1995 by Academic Press, Inc.
All rights of reproduction in any form reserved.

TABLE 1

Crystallization and Crystal Characteristics for the Three $T = 1$ Viruses Whose Structures Have Been Determined Crystallographically

	Crystallization conditions		Crystal characteristics					
Virus	pH	Precipitate	Space group	Unit cell dimensions	Noncryst. symmetry	Resolution of diffraction (Å)	*R* factor	Model
SPMV	7.0	Amm SO_4, 30% saturated	$P4_232$	$a = b = c =$ 183.1 Å	5 subunits (one pentamer)	1.9 Å using image plate and synchrotron radiation	0.21 (30–1.9 Å, $F/\sigma > 3$)	Residues 17–157 and 82 water mol.
STMV	6.5	Amm SO_4, 16% saturated	I222	$a = 174.3$ Å $b = 191.8$ Å $c = 202.5$ Å	15 subunits	1.8 Å using multiwire area detector and crystals grown in microgravity	0.22 (6.0–2.9 Å, $F/\sigma > 5$)	Residues 16–159 and 15 water mol.
STNV	6.5	$MgSO_4$, 1 m*M*	C2	$a = 317.3$ Å $b = 304.0$ Å $c = 184.6$ Å $\beta = 94.4°$	60 subunits (an entire virus particle)	2.5 Å using oscillation photography	0.27 (7.5–2.5 Å, all data)	Residues 12–195 and 148 water mol.

mology at either the amino acid or the nucleotide level with its helper (Pritsch and Mayo, 1989). Only in the 100 to 150 bases at the 3′ ends of the genomic RNAs is there any substantial homology with the RNA of the helper virus, and this is the region of the RNA believed to be bound initially by the helper virus replicase (Joshi and Haenni, 1984).

MATERIALS AND METHODS

Computational techniques

Coordinates of STNV were obtained from the Brookhaven Protein Data Bank, Chemistry Department, Brookhaven National Laboratory (Upton, NY 11973) (Bernstein *et al.,* 1977). Display and analysis of the viral coordinates were carried out with "O" (Jones and Kjeldgaard, 1990) and with X-PLOR Version 3.1 (Brünger, 1992) running on an SGI 340 VGX. Buried area of the molecules was calculated with the program MS (Connolly, 1983) and electrostatic potential of the accessible surface of the molecule by GRASP (Nicholls *et al.,* 1991). Pairwise interactions were calculated using S. Sheriff's program CONTACSYM with standard van der Waals radii (Gelin and Karplus, 1979). Secondary structure predictions for the single-stranded RNA genomes were performed with the program FOLD (Devereux *et al.,* 1984) employing the algorithm of Zucker and Stiegler (1981). Stereochemical quality of a model was analyzed with PROCHECK (Laskowski *et al.,* 1993). Figures were generated by MOLSCRIPT (Kraulis, 1991), "O", and GRASP.

RESULTS

The structure determinations

Before undertaking any structural comparison it may be useful to review some aspects of the crystallographic analyses. These are summarized in Table 1. It often happens that some similarities or differences may be consequences of technique or sample rather than the structures themselves. For example, crystallization conditions could well affect the nature of ions bound or the dispositions of side chains.

The structure of STNV was solved from a monoclinic crystal having the entire virus particle as the asymmetric unit and grown from 1 m*M* $MgSO_4$ at pH 6.5. The data were collected with a conventional laboratory source on photographic film using oscillation cameras. The structure was determined by multiple isomorphous replacement and real space averaging within the asymmetric unit (Liljas *et al.,* 1982). It was refined by restrained least-squares procedures with maintenance of strict icosahedral symmetry. While the capsid proteins were very well resolved and unambiguous, no RNA was observed on the interior of the virus. This was as expected, because there was no reason to believe that the RNA, even if associated with the coat proteins, should assume a distribution compatible with the $T = 1$ icosahedral symmetry of the capsid. It should, however, be noted that low-angle neutron scattering studies based on H_2O/D_2O matching indicated RNA to be organized as helical segments and disposed along the edges of the icosahedron (Bentley *et al.,* 1987).

The structure of SPMV was solved from cubic crystals grown at 4° from 45% saturated ammonium sulfate at pH 7.0. These crystals contained two virus particles in the unit cell, but, because of the high symmetry, had only a pentamer of the capsid proteins as the asymmetric unit. Multiple isomorphous replacement with data collected on a multiwire area detector system and conventional rotating anode source was used for the structure solution, but for high-resolution refinement to 1.9 Å resolution synchrotron data were employed (Ban and McPherson, 1995). As was the case with STNV, the electron density maps of SPMV revealed no ordered binding of RNA to the capsid protein.

The structure of STMV was solved by methods similar to those used for STNV and SPMV but from orthorhombic

crystals grown at room temperature from 15% saturated ammonium sulfate. These had one-fourth, or 15, capsid subunits as the asymmetric unit (Larson *et al.,* 1993b). Multiwire area detector data with a conventional rotating anode source were used for both structure solution and refinement (S. B. Larson and A. McPherson, unpublished results). The 1.8 Å data for the latter, however, were collected from unusually large crystals grown in microgravity (Day and McPherson, 1992).

A striking and unique result was obtained in the analysis of STMV. The electron density map in this case clearly showed the presence of RNA bound to the capsid protein. This RNA appeared as 7-bp segments of double-helical RNA with an additional stacked base at either 3′ terminus. The double-helical segments were closely associated with coat protein dimers in such a way that the icosahedral twofold axes were coincident with dyad axes of the helical segments of RNA. Their orientation along the icosahedral edges, and distribution on the interior of the protein capsid, were consistent with $T = 1$ icosahedral symmetry. In total, about 45% of the RNA of STMV was visualized in the structure.

Comparison of the monomer structures

As it is clear from Fig. 1, the major feature common to the coat proteins of the three viruses is the eight-stranded "jelly-roll" β-barrel that forms the core of each. It occupies the C-terminal portion of the proteins for STNV and STMV and the central portion of the polypeptide in the case of SPMV. Other than that, the shapes, sizes, and general arrangement of the strands in the three monomers are completely different. STMV and SPMV coat proteins are more similar to each other than either is to STNV but when paired with one another their features are not remarkably similar.

The orientations and dispositions of the β-barrels with respect to the icosahedral axes are also quite different for the three viruses. STNV capsid protein, for example, is rotated almost 70° around the long axis with respect to the STMV and SPMV monomers (Fig. 2). There is also a significant difference in the angle that the long axis of the jelly roll forms with respect to the fivefold axes of symmetry. The only similarity that can be observed is that the narrow points of the subunits in all three cases point toward the fivefold axes of symmetry. This we found surprising if there was to be a distinct structure–function relationship ascribed to the β-barrels, vis-à-vis capsid architecture. The dissimilarity, however, readily explains the failure of any one virus to provide a sufficiently precise model for any other as far as molecular replacement approaches to X-ray structure determination were concerned.

The only other feature common to the three coat proteins is an (presumably) extended N-terminal polypeptide of more than 16 amino acids that leaves the surface and appears to be buried in the interior of the virus. STNV is the only virus where the amino-terminal strand forms an α-helix which points toward the interior of the capsid. In both STMV and STNV the amino-terminal strands containing the basic residues enter the core of the capsid close to the icosahedral threefold axes of symmetry. This is true for many $T = 3$ viruses as well, although in $T = 3$ viruses the icosahedral threefold axis is coincident with the quasisixfold axis. Thus in the case of $T = 1$ viruses the N-terminus goes into the interior of the viral particle at the wide end of the jelly roll (threefold axes of symmetry) and in $T = 3$ particles it disappears internally at the narrow end of the jelly roll where quasisixfold axes are located. The N-terminal region of the $T = 3$ capsid protein is also frequently the molecular switch that differentiates fivefold and quasisixfold axes (Rossmann and Johnson, 1989). It is not the case, however, for SPMV. Here the electron density of the amino-terminal strand disappears in the proximity of the twofold axis of icosahedral symmetry. This implies that if the arrangement of RNA in the interior of the three viruses is very similar, then the interaction of the amino-terminal strand of SPMV with the RNA is quite different from that of the other two viruses. Conversely, if the amino-terminal strands make the same interactions in all three viruses then it means the RNA is arranged differently for SPMV than for the other satellite viruses.

In all three cases, the 16 amino acids of the amino termini include at least five basic residues; STMV—2 Arg and 3 Lys, STNV—3 Arg and 2 Lys, and SPMV—1 Arg and 6 Lys. In all cases the basic amino acids are assumed to interact with and neutralize negatively charged phosphates of the RNA. The SPMV capsid can neutralize 92% of the negatively charged phosphates of the RNA in the interior, while the STNV capsid, containing 1239 nucleotides, can only neutralize 72% of the phosphates of the RNA. This suggests that there is a significant excess of negative charge within STNV that must be neutralized by other ions or polyamines.

The volumes available to RNA are 1.4 and 1.6 times larger for STMV and STNV compared with SPMV, but the amount of RNA is 1.2 and 1.5 times greater than the amount of RNA in SPMV. Comparing the inner surface area of the capsids, however, we find STMV 1.2 times greater and STNV 1.4 times greater than SPMV. This implies that, in the case of these three $T = 1$ viruses, envelopes which are required to pack more nucleic acid do this by proportionately increasing the inner area of the capsid. This, however, results in increased dead space at their core. This may reflect a requirement for nucleic acid to interact with the capsid during viral assembly.

The dimer structures

The capsid dimers of STMV, STNV, and SPMV, presented in Fig. 3, do not resemble one another in terms

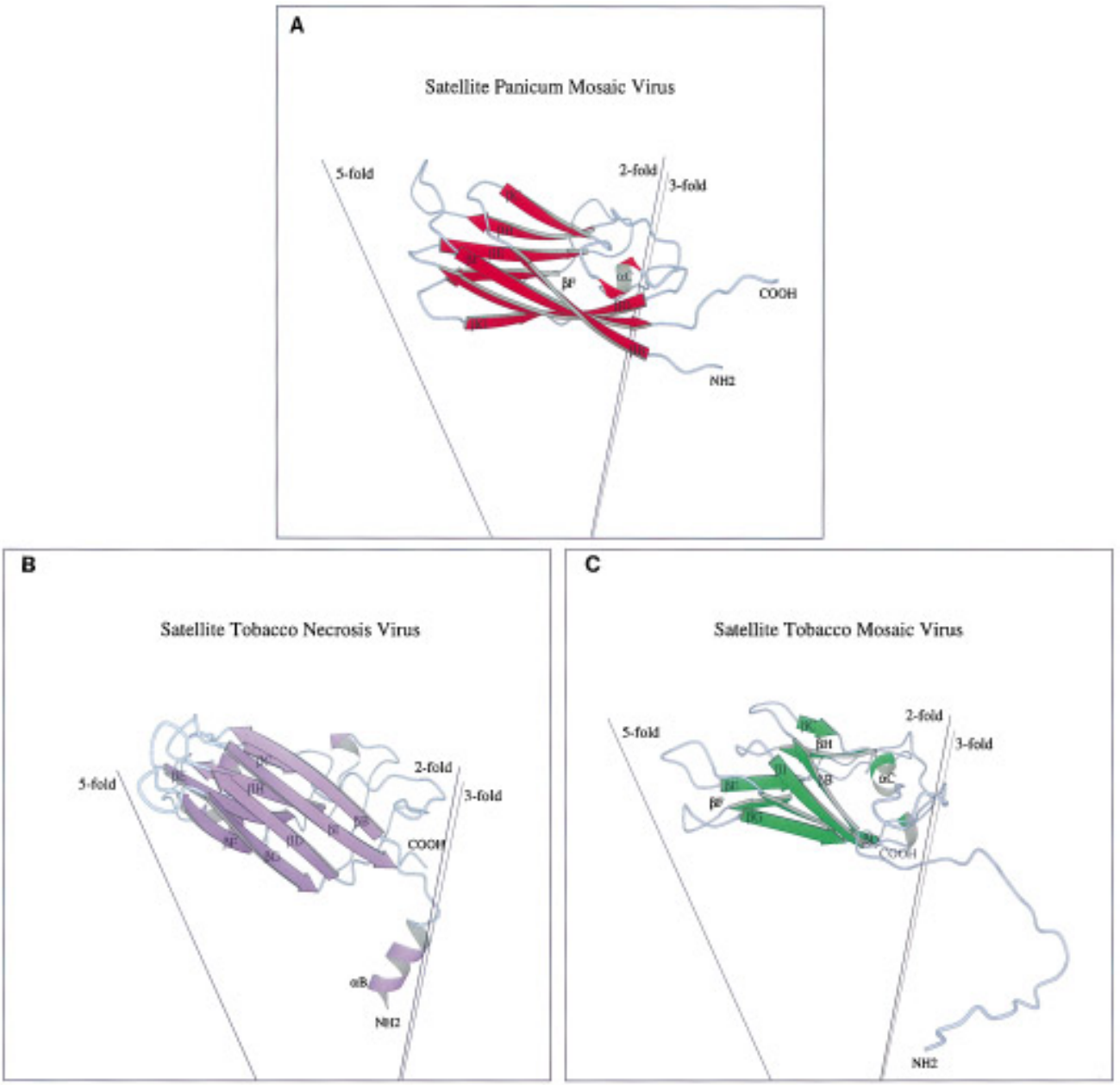

FIG. 1. Ribbon diagrams of individual subunits of the coat proteins of three satellite viruses shown with respect to the icosahedral axes of symmetry. The capsid proteins are composed of an eight-stranded jelly-roll β-barrel and an extended amino-terminal helix in the case of STNV, an extended amino-terminal strand in the case of STMV, and an extended carboxy-terminal strand in the case of SPMV. The figure was generated by MOLSCRIPT (Kraulis *et al.,* 1991).

of interfaces or their extent, interactions, or orientations with respect to the icosahedral dyad axes. The dimer of STMV represents a very close association with intricate bonding interactions over a large buried surface area of 1780 A^2 (Table 2). The amino-terminal polypeptides of the two embrace one another and form additional strands to the β-barrels of the other. At the immediate interface are prominent, symmetry-related, tryptophan stacking interactions and numerous cooperative contacts with the nucleic acid. In STMV, the dimer is surely the structural and assembly unit of the capsid.

In SPMV, on the other hand, the dimer interface buries only 640 A^2 and is otherwise very simple and sparse. Amino acids belonging to the first β-strand (B) of the monomer form a β-ribbon with a symmetry mate across the dyad and make the β-sheet of one contiguous with the other. This is similar to the continuous sheet structures formed by the Southern bean mosaic virus and tomato bushy stunt virus (Rossmann *et al.,* 1983) around their icosahedral twofold axes. This interface is tenuous and it appears that it could be easily disrupted. There are relatively few contacts between twofold related monomers.

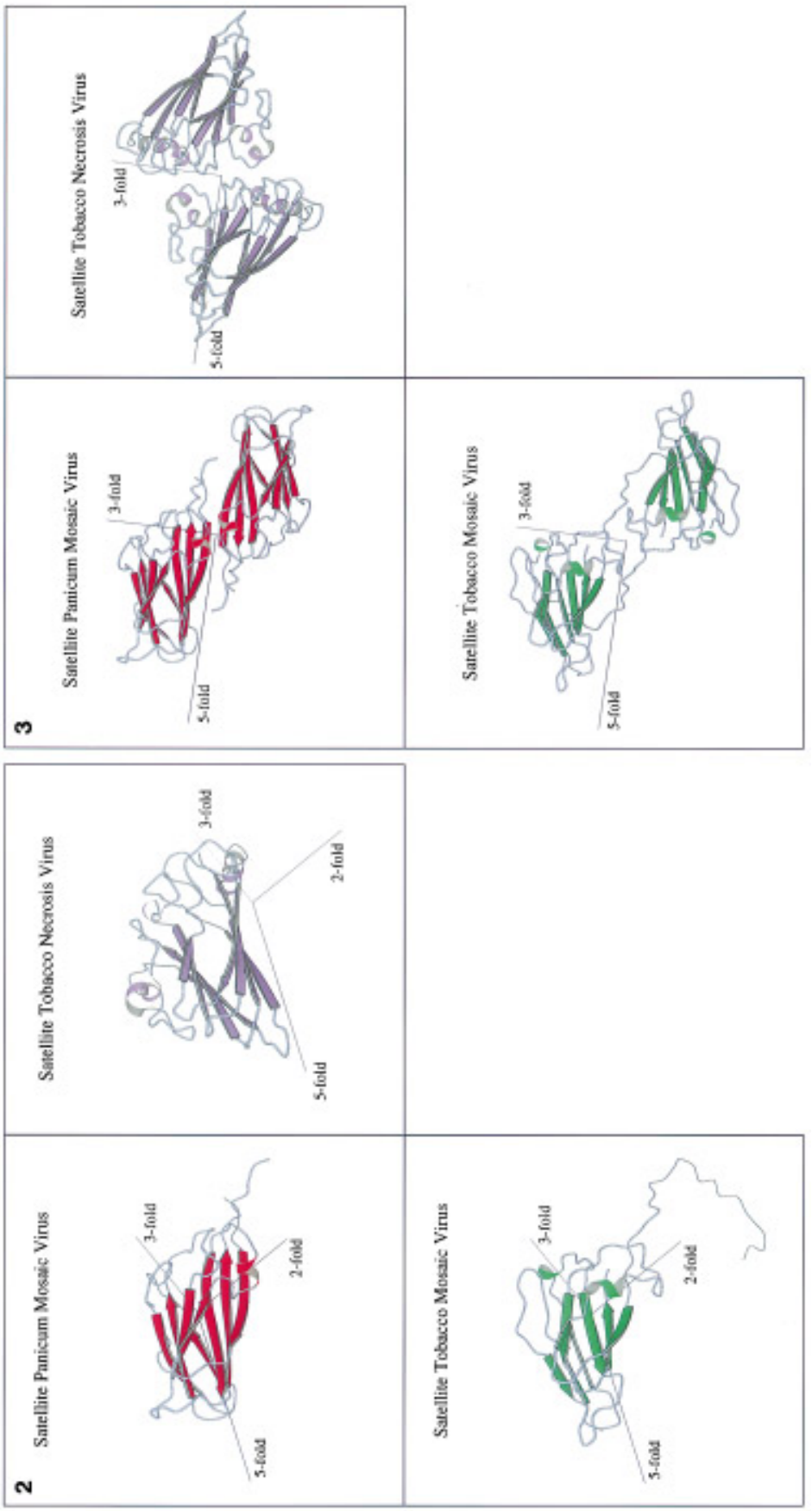

FIG. 2. The viral protein monomers viewed from the exterior of the virus showing their relationship to the icosahedral axes of symmetry. There is a large difference in the rotation angle about the fivefold axis of symmetry between STNV and the other two viruses. The STNV subunit is, furthermore, rotated around its long axis by approximately 70°.

FIG. 3. Twofold capsid protein interactions for the three satellite viruses. STMV in this comparison shows the greatest area of interaction. This is primarily because of long amino-terminal strands which extend around a twofold related monomer and disappear into the interior of the particle near the threefold axis of symmetry.

TABLE 2

(A) Intersubunit Buried Surface Area

Category	Subunit	Area (Å^2)	%	NRES	NATM
SPMV 2 mer		639.5	50.0	28	77
SPMV 3mer	2–1	773.1	49.3	24	96
SPMV jelly roll	2–1	451.7	28.8	16	62
SPMV C-term	2–1	321.4	20.5	8	34
SPMV 3mer	1–2	796.1	50.7	35	104
SPMV 5mer	1–2	493.1	47.0	17	60
SPMV 5mer	2–1	555.4	53.0	19	59
STMV 2mer	1–2	1782.3	50.1	56	224
STMV 2mer beta	1–2	727.7	20.4	19	90
STMV 2mer jelly	1–2	1054.6	29.6	37	134
STMV 3mer	1–2	653.5	49.5	22	81
STMV 3mer	2–1	666.9	50.5	23	81
STMV 3mer beta	2–1	286.1	21.7	8	33
STMV 3mer jelly	2–1	380.8	28.8	15	48
STMV 5mer	1–2	405.8	48.7	14	52
STMV 5mer	2–1	427.5	51.3	16	57
STNV 2mer		647.1	50.2	23	75
STNV 3mer	1–2	610.8	51.2	19	77
3mer alpha term	1–2	286.5	24.0	8	33
3mer jelly roll	1–2	348.3	29.2	12	48
STNV 3mer	2–1	581.9	48.8	25	85
3mer alpha term	2–1	207.4	17.4	9	28
3mer jelly roll	2–1	400.3	33.6	17	59
STNV 5mer	1–2	850.4	49.9	33	106
STNV 5mer	2–1	852.4	50.1	34	102
5mer alpha term	2–1	219.6	12.9	9	27
5mer jelly roll	2–1	663.3	39.0	26	76

(B) Intersubunit Interactions

Category	Subunit	NRES	NATM	NHBD	SLT	NVDW
SPMV 2mer		13	32	14	2	39
SPMV 3mer	2–1	23	81	18	2	188
SPMV jelly roll	2–1	15	55	9	2	119
SPMV C-term	2–1	8	26	9	2	69
SPMV 3mer	1–2	28	85	18	2	188
SPMV 5mer	1–2	14	40	6	0	77
SPMV 5mer	2–1	12	36	6	0	77
STNV 2mer		17	58	6	4	131
STNV 3mer	1–2	12	36	6	0	69
STNV N-term	1–2	6	14	0	0	30
STNV jelly roll	1–2	6	22	6	0	39
STNV 3mer	2–1	13	38	6	0	69
STNV N-term	2–1	4	12	1	0	19
STNV jelly roll	2–1	9	26	6	0	50
STNV 5mer	1–2	21	57	8	2	104
STNV 5mer	2–1	20	51	8	2	104
STMV 2-mer		41	145	20	0	316
STMV N-term		16	62	8	0	124
STMV jelly roll		25	83	12	0	192
STMV 3mer	1–2	16	56	12	0	98
STMV 3mer	2–1	18	52	12	0	98
STMV N-term	2–1	8	26	4	0	47
STMV jelly roll	2–1	10	26	8	0	51
STMV 5mer	1–2	11	40	8	4	75
STMV 5mer	2–1	9	38	8	4	75

Note. Intersubunit buried surface area and contacts for the three viruses with a breakdown for the core of the monomer and a 7-amino-acid carboxy-terminal extension for SPMV, 19 amino-terminal amino acids which form an extension for STMV, and 12 amino acids which constitute amino-terminal helix in STNV. This was done only when these secondary structural elements were involved in contacts. NRES and NATM indicate number of residues and number of atoms, respectively, participating in interactions between subunits. (A) Buried surface area was calculated using Connolly's algorithm with a 1.7 Å radius probe. Percentages are of the total buried area between the two interacting subunits indicated in the column on the left. (B) Van der Waals contacts are shown (column NVDW), for which the maximum interatomic distance is 4.11 Å, and probable hydrogen bonds (column NHBD), for which the maximum distance between electronegative atoms is 3.5 Å (selected according to the geometry as well as the distance criterion); maximal distance for a salt link is 3.8 Å (column SLT). When nonsymmetric interactions occur, in trimers and pentamers, the number of hydrogen bonds provided by each surface is assigned: molecule 1–2 and molecule 2–1. The contacts which are mediated through water molecules and metal ions are not listed in this table. Metal ions add to the strength of interaction in the case of STNV where there are two Ca^{2+} ions between trimers and one at the fivefold axis of symmetry.

For STNV the interaction between twofold related subunits is stabilized by a pair of salt links and 650 Å^2 of buried surface area. This is the most extensive interface in STNV with regard to the number of van der Waals contacts. Because of the different orientation of subunits in this virus this interface is generated primarily by the loops following the βG-strand and loops between the βE and βF strands.

The trimer structures

For STMV and STNV the trimer interactions, illustrated in Fig. 4, are significant but not exceptional. Of the surface area, 650 A^2 and 610 A^2, respectively, are buried, and there are 12 and 6 hydrogen bonds, respectively, mediating the contacts. The residues surrounding the threefold icosahedral axes in STMV are provided by the short helical loop immediately following the βG strand. Helices at the amino-terminal region of STNV form three helix bundles pointing toward the interior of the capsid, presumably interacting with the RNA. There are also two metal ions found at the threefold interface of STNV which add to the total number of hydrogen bonds at this interface. For SPMV, the threefold contacts are considerably more extensive with almost 800 A^2 of buried surface, 188 van der Waals contacts, 18 hydrogen bonds, and 2 salt linkages per interface. This is primarily due to the extended carboxy-terminal peptide which is responsible for 44% of the total buried area between trimers. This strand extends toward the surface of the virus on the outer side of the trimer. As was true with the icosahedral twofold axes, the dispositions of the core β-barrels in the three viruses with respect to the icosahedral threefold axes are completely different in the three capsid shells.

The pentamer structures

Pentameric interactions, presented in Fig. 5, are by far the most extensive and intricate for STNV, and based on this feature alone, the pentameric unit could serve as the organizing unit in assembly. The pentamers are capped on the symmetry axes by Ca^{2+} ions liganded by the carbonyl oxygens of Thr138 and two water molecules. This contributes additional rigidity and stability. In the pentamer from STMV, on the other hand, there is also an ion on the fivefold axis, but it is almost certainly an anion coordinated by Asn115 and Asn117. In this pentamer, however, there are few other contacts and only a sparse network of hydrogen bonds. In STMV, therefore, the pentameric assembly does not appear to be a crucial structural unit. Interactions between pentameric subunits in SPMV are similar in terms of buried surface area and hydrophobic contacts to STMV. SPMV has no ions on its fivefold axes, and there are no salt links between fivefold related subunits. As was true for the icosahedral two- and threefold axes, there is no correspondence between the orientations of the β-barrel cores of the capsid proteins with respect to the fivefold axes of symmetry. For example, a monomer in STNV is rotated approximately 35° around the fivefold axis when compared with an equivalent SPMV monomer.

The viral capsids

The capsids of STNV, STMV, and SPMV are shown in Fig. 6. The capsid of SPMV is the smallest. The entire virus viewed down the fivefold axis of icosahedral symmetry has loops which gather to form a pronounced crown arrangement that gives the appearance of a slight puckering. A similar protrusion which forms a cusp is pronounced in STNV, giving the virus an obvious icosahedral shape, but this is virtually absent in STMV. The cusp on the fivefold axis in STNV could be a consequence of the significantly different orientation of the protein subunits with respect to the icosahedral axes as discussed above. From the graph in Fig. 7, it can be deduced that the outer diameters for SPMV, STMV, and STNV are approximately 160, 166, and 180 Å, and that the inner diameters for the three viruses are approximately 114, 126, and 136 Å.

The distribution and orientation of protein monomers in the three $T = 1$ viruses are considerably different. An interesting comparison can be made in terms of the extent of interactions such as buried surface area, number of contacts, hydrogen bonds, and salt links between twofold, threefold, and fivefold related subunits of the three viruses. This is summarized in Table 2. It should be pointed out, however, that this summary does not take into account interactions generated by water molecules and metal ions.

The nucleic acid

Of the three satellite viruses, only in STMV was RNA ordered and clearly visible. This was visualized as 30 segments of double-stranded helical RNA of 7 bp with additional stacked bases at the 3′ termini of each strand in the duplex. The central dyad axis of each RNA duplex was coincident with that of the protein dimers and the icosahedral twofold axes. In all nearly 45% of 1059 bases of the STMV RNA genome was visible. This remains the most nucleic acid yet seen in the interior of any virus.

In neither STNV nor SPMV was RNA clearly visible in the electron density maps, though in the case of SPMV some suspect RNA was detected in the neighborhood of the pentameric axis. While no RNA was visualized in STNV by X-ray diffraction, neutron scattering did reveal the presence, at low resolution, of RNA. This was interpreted as short double-helical segments of RNA aligned along the icosahedral edges. Remarkably, this was essentially the same arrangement seen at high resolution in the X-ray diffraction structure of STMV. Thus, there is some reason to believe that, at least for STMV and STNV,

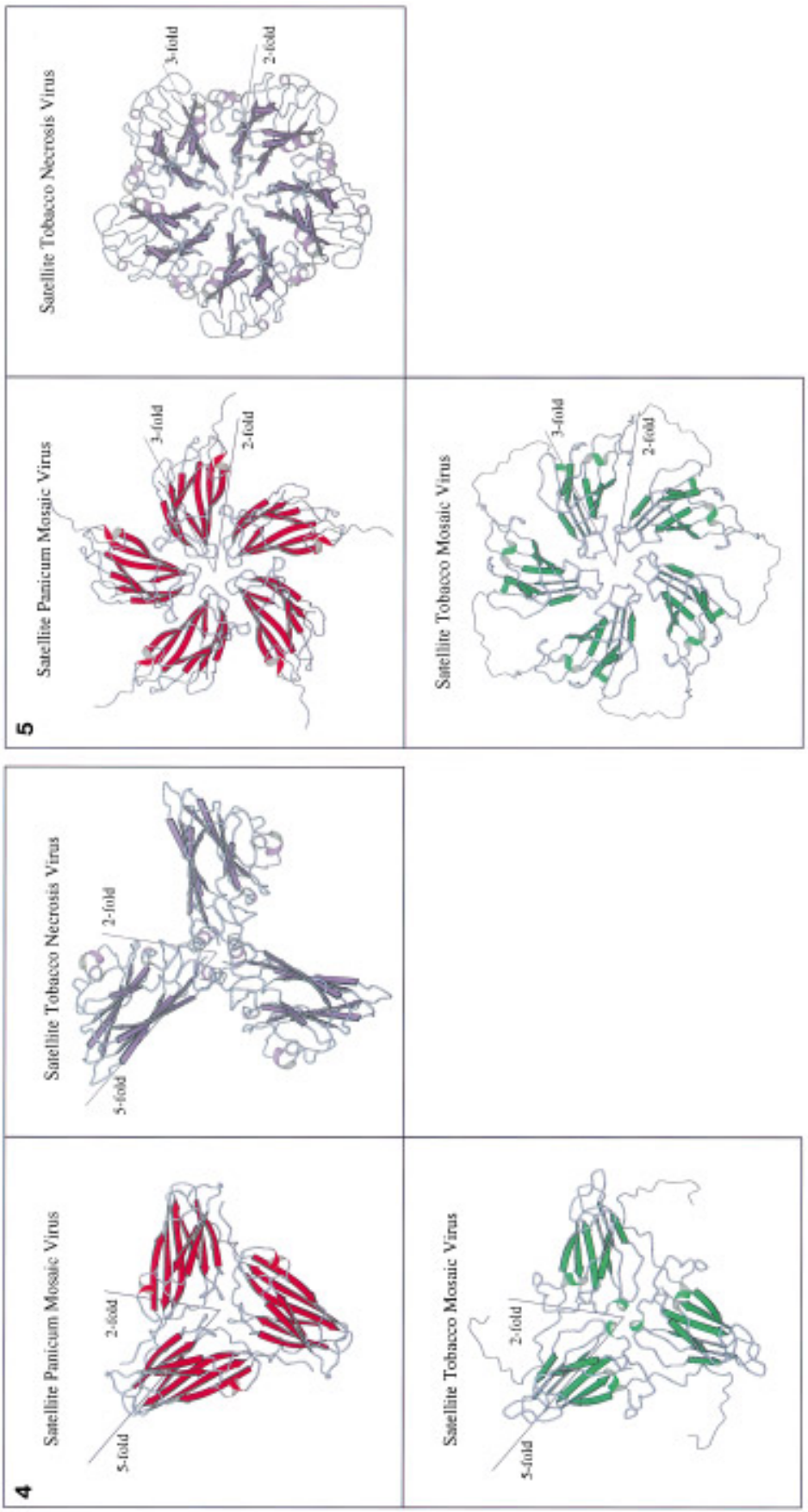

FIG. 4. Threefold interactions for the three viruses. The interaction is most intricate for SPMV because of the extended carboxy-terminal strand which originates at the interior of the capsid and extends toward the fivefold axis of icosahedral symmetry on the exterior of the capsid. The amino-terminal helices are primarily responsible for threefold interactions in the case of STNV. Two calcium ions participate in the threefold interactions for STNV.

FIG. 5. Fivefold capsid protein interactions for the three satellite viruses. These interactions are most extensive for STNV. The STNV capsid also has a cation at the fivefold axis of symmetry, while the STMV pentamer has an anion there.

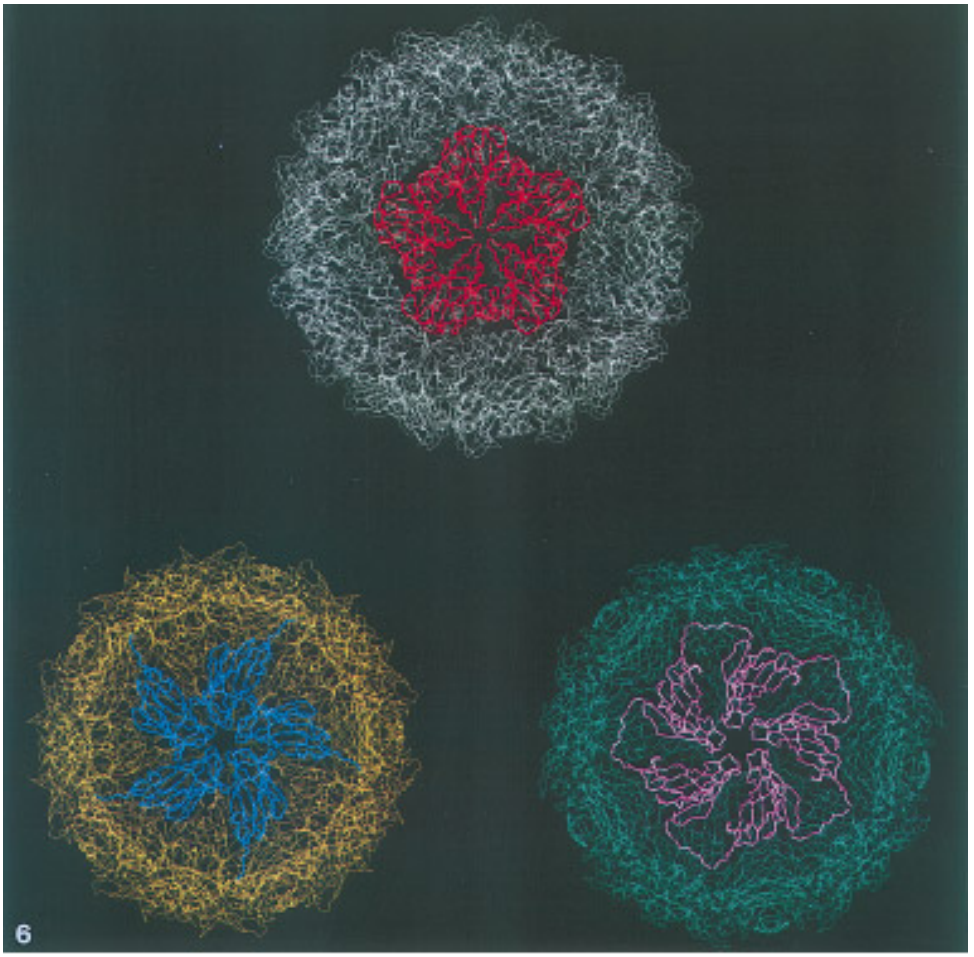
6

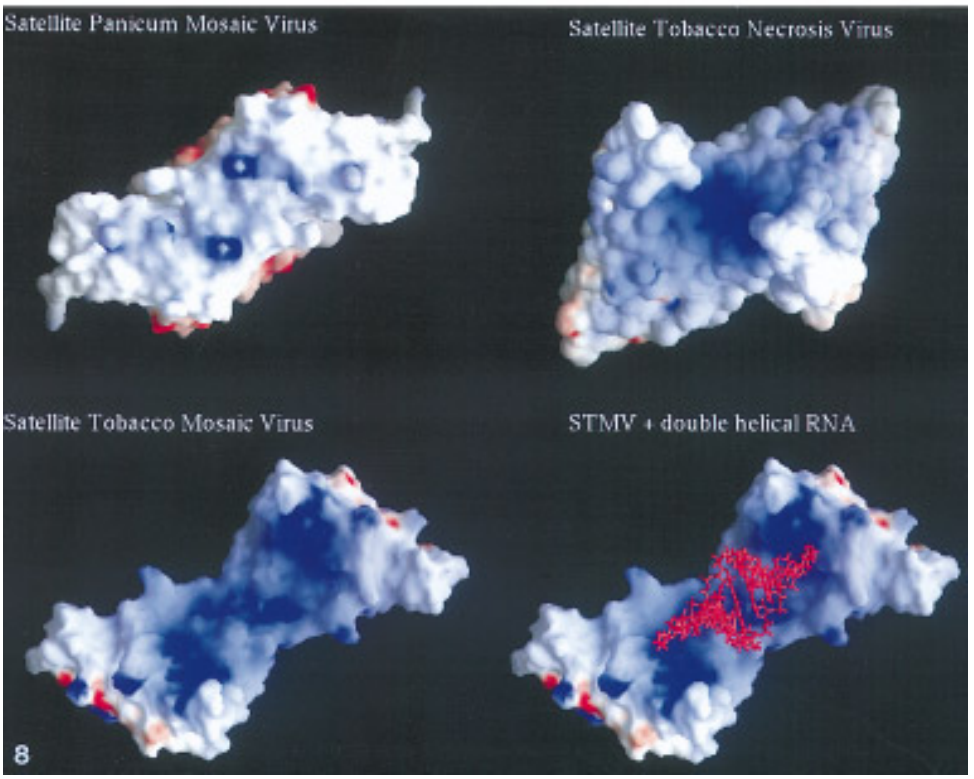
Satellite Panicum Mosaic Virus
Satellite Tobacco Necrosis Virus
Satellite Tobacco Mosaic Virus
STMV + double helical RNA
8

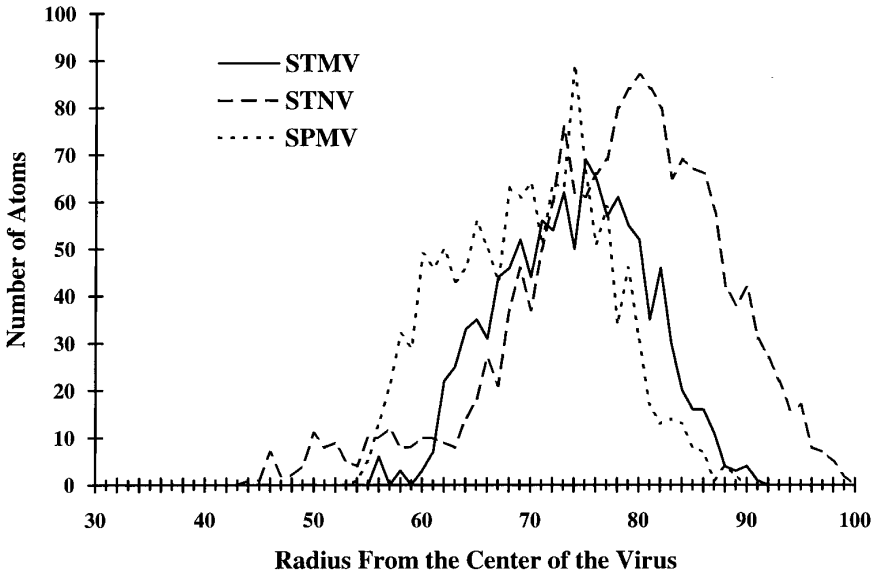

FIG. 7. Graph of the number of atoms as a function of distance from the viral center for the three viruses. The average inner and outer radii of the viral capsid can be taken as half the maximum height of the curve on the inside and the outside of the capsid, respectively.

the conformation and packing of RNA in the interior of the capsid may be similar.

Examination of the electrostatic surfaces exposed by each STMV dimer to the double-helical RNA might indicate whether similar regions exist in the other two viruses. Interestingly, the STMV dimer does posses a characteristic pattern, in the shape of a reversed letter S, of positively charged surface oriented toward the interior of the virus. A similar pattern is not observed in STNV and SPMV. This is shown in Fig. 8. Examining a larger inner surface of the three viruses with respect to electrostatic potential reveals that both STNV and SPMV have highly positively charged surfaces on the interior of their pentamers. This is the region where fivefold averaged density which could be assigned to RNA was located in the crystallographic studies of STNV and SPMV (Liljas *et al.,* 1982; Ban and McPherson, 1995).

DISCUSSION

Although the three satellite viruses appear superficially similar in many regards, the salient feature of this comparison is the striking dissimilarity that characterizes them at a more detailed level. The comparison of the three $T = 1$ viruses on a biochemical and structural level is summarized in Table 3. Considering the structural and biochemical differences, it is not unreasonable to propose that the assembly pathways of the three viruses may be different as well. In STMV the prominent electrostatic and stereochemical complementarity between coat protein dimers and segments of double-helical RNA on the interior immediately suggest that assembly of STMV involves close, coordinated, and probably cooperative interaction between the RNA and the coat protein. The absence of such features for STNV and SPMV suggest protein–nucleic acid interactions may be less pronounced. It should be noted, however, that no instance of "empty heads" for any of these three viruses has been reported. In addition, double-helical RNA has been postulated to be associated with capsid protein of STNV based on low-angle neutron diffraction studies. These indicate that, even though not as prominent as in STMV, protein RNA interactions may play some role in assembly of STNV and SPMV.

The inner electrostatic surfaces of dimers, trimers, and pentamers, all possible assembly intermediates, and the physical interfaces between monomers within the capsid further suggest that the assembly sequences and mechanisms might be more diverse. For STMV the dimer is almost certainly the crucial unit for construction, for

FIG. 6. The three viral capsids viewed along an icosahedral fivefold axis of symmetry. Only Cα atoms are shown for clarity. One pentamer on the surface of the virus is shown in a different color. The three viruses are drawn to scale. STNV is the largest, shown in white and red. The smallest virus, SPMV, shows an obvious crown-like arrangement of loops around the fivefold axis, giving it a unique appearance. It is displayed in bottom left in gold and blue. Extended amino-terminal strands are obvious in STMV at bottom right shown in purple and cyan. Figure was generated by "O" (Jones and Kjeldgaard, 1990) and displayed on an SGI 340 VGX workstation.

FIG. 8. The interior surface of the viral protein dimers colored according to the electrostatic potential; positive potential is indicated by blue, negative in red. The bottom two representations are both from STMV, one with and one without the double-helical RNA. The RNA is shown as a stick model in red consistent with the negative charge of the RNA phosphates. The surface was calculated by GRASP (Nicholls *et al.,* 1991) and displayed on an SGI 340 VGX workstation.

SPMV the trimer is more likely, and for STNV the pentamer appears to be the most cohesive unit. In each case these oligomers maintain the greatest surface contact area and electrostatic and stereochemical complementarity, maintain the most intricate bonding arrangements, and present the most attractive surfaces to the nucleic acid.

Disassembly, too, may take place by different pathways. It has been suggested that for some viruses removal of Ca^{2+} from the capsid could cause dissociation of the capsomers (Durham *et al.,* 1977). While this is possible for STNV, it clearly cannot be the case for either STMV or SPMV, which lack Ca^{2+}. In fact, it is unlikely that any fivefold "linchpin mechanism" exists, Ca^{2+} or otherwise, for these two satellite viruses.

Given the propensity for economy displayed by most viruses, a reasonable question is why the satellite viruses contain even more nucleic acid than is required to effect replication and code for the amino acid sequence of the coat protein. This amount of "extra" RNA ranges from 380 nucleotides for SPMV to 580 and 650 nucleotides for STMV and STNV, respectively.

It might well be that the additional RNA is needed to provide a structural framework for the capsid, or to effect a temporal and spatially ordered addition of protein subunits to the RNA during assembly. Perhaps the RNA has a dual coding responsibility, its sequence providing a genetic function vis-à-vis the coat protein, its secondary structure a code for the ordered assembly of the virus. That is, the RNA serves an additional role, as it probably does in the assembly of ribosomes, as an organizational framework whose presentation of binding sites directs assembly. This would explain the excess of RNA and at the same time restore viral respect for molecular thrift and efficiency.

Some common structural features of the satellite viruses, such as the β-barrels of the coat proteins, suggest an evolutionary relationship, but there seems to be lacking any unifying principle that implies either divergence from a common source or convergence to a common motif. The latter hypothesis seems particularly unlikely because the major structural features of the coat proteins, the β-barrels, are so dissimilar in detail and disposition within the icosahedra. In addition to the lack of sequence homology between viruses, the locations of the eight β-sheet strands with respect to the linear amino acid sequence of the protein are, as indicated in Fig. 9, very different.

Plant viruses in the wild, however, often coinfect the same host and in doing so generate genetic recombinants. This process could provide a mechanism for the genesis of the $T = 1$ viruses. One could postulate that the satellite viruses may have originated by splicing together elements of the genomes of various $T = 3$, or $T = N$, naturally occurring plant viruses, taking a piece of the coat protein here, a replicase binding site there, etc. This hybrid, abbreviated genome could then produce a packaging coat, a protein resembling one virus, while establishing a different helper virus relationship based on the replication binding site of another. Such a virus could mutate rapidly, while preserving the core topology, so that it did not show homology with the virus that it originated from, nor the new helper. This is particularly likely for RNA viruses since the rate of change for RNA genes far exceeds the rate of change for DNA genes (Holland *et al.,* 1982). This would explain both the lack of homology or immuno-cross-reactivity with the helper virus and how the β-barrel protein core arose at the same time.

Satellite viruses then, in an evolutionary sense, might be hybrid structures composed of bits and scraps of larger, more complex viruses. If this is the case, then additional satellite viruses may be continuously created in the wild and their ability to survive tested by the environment.

Of the three satellite viruses analyzed by X-ray diffrac-

TABLE 3

Structural and Biochemical Comparison between Four $T = 1$ Viruses

Virus	T	M_r (daltons)	Diameter (Å)	Helper virus	Host plant	Genome size	Coat protein	Ion on fivefold	3′tRNA	Resolution structure (Å)	RNA visible
STNV	1	1.67×10^6	180	Tobacco necrosis virus (icos.)	Tobacco	1239 bases M_r 415,000	195 aa M_r 21,000	Ca^{2+}	No	2.5 Å	No
STMV	1	1.40×10^6	166	Tobacco mosaic virus (rod)	Tobacco	1059 bases M_r 350,000	159 aa M_r 17,500	anion (SO_4^{2-})	Yes (His)[a]	1.8 Å	Yes (~45%)
SPMV	1	1.30×10^6	160	Panicum mosaic virus (icos.)	Millet	825 bases M_r 275,000	157 aa M_r 17,000	None	No	1.9 Å	No
SMW LMV	1	1.84×10^6	ND[b]	Maize white line mosaic virus (icos.)	Maize	1168 bases M_r 389,000	208 aa M_r 24,000	ND	ND	ND	ND

[a] The tRNA-like structure was biochemically proven for STMV (Felden *et al.,* 1994).

[b] ND, not determined.

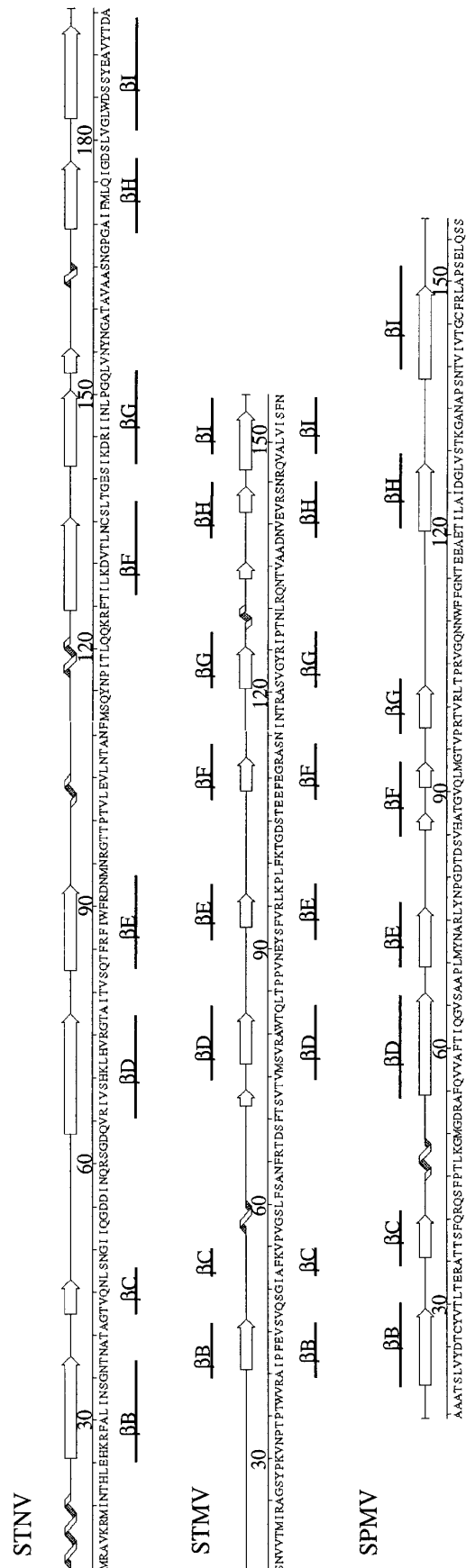

tion analysis, STMV seems most unique. Of the three, the capsid of STMV seems most intricately woven and exhibits the most substantial interfaces between subunits. The RNA is systematically organized and packaged in the capsid so that it obeys icosahedral symmetry. The remarkably close interaction of the dimers of coat protein suggest an assembly pathway involving sequential, cooperative, perhaps programmed complexation of protein and nucleic acid. Neither STNV nor SPMV exhibit these properties.

ACKNOWLEDGMENTS

This research was sponsored by grants from the National Aeronautics and Space Administration, the National Institutes of Health, and the National Science Foundation. The authors thank Professor Alan Dodds for valuable discussions and Mr. Aaron Greenwood and Mr. John Day for their technical assistance. We thank the Academic Computing Graphics and Visual Imaging Lab, University of California, Riverside, for help in generating figures.

REFERENCES

Ban, N., and McPherson, A. (1995). The structure of satellite panicum mosaic virus at 1.9 Å resolution. *Nat. Struct. Biol.,* in press.

Bentley, G. A., Lewit-Bentley, A., Liljas, L., Skoglund, U., Roth, M., and Unge, T. (1987). Structure of RNA in satellite tobacco necrosis virus: A low resolution neutron diffraction study using $^1H_2O/^2H_2O$ solvent contrast variation. *J. Mol. Biol.* 194, 129–141.

Bernstein, F. C., Koetzle, T. F., Williams, G. J. B., Meyer, E. F., Jr., Brice, M. D., Rodgers, J. R., Kennard, O., Shimanouchi, T., and Tasumi, M. (1977). The protein databank: A computer-based archival file for macromolecular structures. *J. Mol. Biol.* 112, 535–542.

Brünger, A. T. (1992). X-PLOR Manual, Version 3.1, Yale University, New Haven, CT.

Caspar, D. L., and Klug, A. (1962). Physical principles in the construction of regular viruses. *Cold Spring Harbor Symp. Quant. Biol.* 27, 1–24.

Connolly, M. L. (1983). Analytical molecular surface calculation. *J. Appl. Crystallogr.* 16, 548–558.

Day, J., and McPherson, A. (1992). Macromolecular crystal growth experiments on International Microgravity Laboratory-1. *Protein Sci.* 1, 1254–1268.

Day, J., Ban, N., Patel, S., Larson, S. B., and McPherson, A. (1994). Characterization of crystals of satellite panicum mosaic virus. *J. Mol. Biol.* 238, 849–851.

Devereux, J., Haeberli, P., and Smithies, O. (1984). A comprehensive set of sequence analysis programs for the VAX. *Nucleic Acids Res.* 12, 387–395.

Dodds, J. A. (1991). Structure and function of the genome of satellite tobacco mosaic virus. *Can. J. Plant Pathol.* 13, 192–195.

Durham, A. C. H., Hendry, D. A., and Von Wechmar, M. B. (1977). Does calcium ion binding control plant virus disassembly? *Virology* 77, 524–533.

Felden, B., Florentz, C., McPherson, A., and Giege, R. (1994). A histidine

FIG. 9. Secondary structure assignments calculated from the crystallographically determined structures of the three viruses. Locations of the eight β-sheet strands forming the conserved jelly-roll topology of the core of the monomer were determined from the three-dimensional arrangement of the secondary structural elements of the subunits. There is no obvious homology in terms of either sequence or the positions of secondary structural elements in these viruses.

accepting tRNA-like fold at the 3′-end of satellite tobacco mosaic virus RNA. *Nucleic Acids Res.* 22, 2882–2886.

Francki, R. I. B. (1985). Plant virus satellites. *Annu. Rev. Microbiol.* 139, 151–174.

Gelin, B. R., and Karplus, M. (1979). Side chain torsional potentials: Effect of dipeptide, protein and solvent environment. *Biochemistry* 8, 1256–1268.

Holland, J., Spindler, K., Horodyski, F., Grabau, E., Nichol, S., and Vande Pol, S. (1982). *Science* 215, 1577–1585.

Jones, A. T., and Liljas, L. (1984). Structure of satellite tobacco necrosis virus after crystallographic refinement at 2.5 Å resolution. *J. Mol. Biol.* 177, 735–767.

Jones, T. A., and Kjeldgaard, M. (1990). "O" Manual, Version 5.4, Uppsala University, Sweeden and Aarhus University, Denmark.

Joshi, S., and Haenni, A.-L. (1984). Plant RNA viruses: Strategies of expression and regulation of viral genes. *FEBS Lett.* 177, 163–174.

Kassanis, B. (1962). Properties and behavior of a virus depending for its multiplication on another. *J. Gen. Microbiol.* 27, 477–488.

Kraulis, P. J. (1991). MOLSCRIPT: A program to produce both detailed and schematic plots of protein structures. *J. Appl. Crystallogr.* 24, 946–950.

Larson, S. B., Koszelak, S., Day, J., Greenwood, A., Dodds, J. A., and McPherson, A. (1993a). Double helical RNA in satellite tobacco mosaic virus. *Nature (London)* 361, 179–182.

Larson, S. B., Koszelak, S., Day, J., Greenwood, A., Dodds, J. A., and McPherson, A. (1993b). Three-dimensional structure of satellite tobacco mosaic virus at 2.9 Å resolution. *J. Mol. Biol.* 231, 375–391.

Laskowski, R. A., MacArthur, M. W., Moss, D. S., and Thornton, J. M. (1993). Procheck — A program to check the stereochemical quality of protein structures. *J. Appl. Crystall.* 26, 283–291.

Liljas, L., Unge, T., Jones, T. A., Fridborg, K., Lovgren, S., Skoglund, U., and Strandberg, B. (1982). Structure of satellite tobacco necrosis virus at 3.0 Å resolution. *J. Mol. Biol.* 159, 93–108.

Masuta, C., Zuidema, D., Hunter, B. G., Heaton, L. A., Sopher, D. S., and Jackson, A. O. (1987). Analysis of the genome of satellite panicum mosaic virus. *Virology* 159, 329–338.

Nicholls, A., Sharp, K., and Honig, B. (1991). Protein folding and association — Insights from the interfacial and thermodynamic properties of hydrocarbons. *Proteins Struct. Funct. Genet.* 4, 281–296.

Pritsch, C., and Mayo. (1989). Sattelites of plant viruses. *In* "Plant Viruses, Vol. I, Structure and Replication" (C. L. Mandahar, Ed.), pp. 289–321. CRC Press, Boca Raton, FL.

Rossmann, M. G., and Johnson, J. E. (1989). Icosahedral RNA — Virus structure. *Annu. Rev. Biochem.* 58, 533–573.

Rossmann, M. G., Abad-Zapatero, C., Murthy, M. R. N., Liljas, L., Jones, A., and Strandberg, B. (1983). Structural comparisons of some small spherical plant viruses. *J. Mol. Biol.* 165, 711–736.

Valverde, R. A., and Dodds, J. A. (1986). Evidence for a satellite RNA associated naturally with the U5 strain and experimentally with the U1 strain of tobacco mosaic virus. *J. Gen. Virol.* 67, 1875–1884.

Zhang, L., Zitter, T. A., and Palukaitis, P. (1991). Helper virus-dependent replication, nucleotide sequence, and genome organization of the satellite virus of maize white line mosaic virus. *Virology* 180, 467–473.

Zucker, M., and Stiegler, P. (1981). Optimal computer folding of large RNA sequences using thermodynamics and auxiliary information. *Nucleic Acids Res.* 9, 133–148.